IOSR Journal of Mechanical and Civil Engineering (IOSR-JMCE)
e-ISSN: 2278-1684,p-ISSN: 2320-334X, Volume 17, Issue 2 Ser. V (Mar - Apr 2020), PP 11-19
www.iosrjournals.org

Structure Analysis of Parallel Robot in Friction Stir Welding Technology

*Nicas January Benard [1], Professor Liu Ying[2]
1(2017/2020), Mechanical Engineering Collage, Tianjin University of Technology and Education (TUTE), China.
**Engineer II, Tanzania Engineering and Manufacturing Design Organization (TEMDO), Tanzania.*
2Lecturer: Mechanical Engineering Collage, Tianjin University of Technology and Education(TUTE), China.

Abstract:*Friction Stir Welding (FSW) processes, parameters vital in friction stir welding and the force in the welding process in combination with the actual engineering application and welding process requirements are analyzed. At the same time, the mechanical structure of parallel robot based on 2UPR/RPS is analyzed, which is designed on consideration of friction stir welding processes, but not limited to the degree of freedom analysis, coordinate system establishment and kinematics analysis.*

Keywords:*Parallel Robot; Friction Stir Welding; Process Parameters; Degree of freedom; Forces*

Date of Submission: 02-04-2020 Date of Acceptance: 18-04-2020

I. Introduction

As a new type of welding technology, friction stir welding can be used for the welding of metal and alloy materials. The selection of suitable welding processes and parameters will directly affect the quality of welding. Friction stir welding does not require other consumables and shielding gas during the welding process, which reduces the weld defects and porosity defects existing in the traditional welding method to a certain extent. At the same time, when welding metal materials, friction stir welding is not required to perform any pretreatment work, so the welding efficiency can be greatly improved[1]–[4].

A suitable welding process requires a suitable welding equipment structure for support in order to achieve good welding quality results. Therefore, in the design of parallel friction stir welding robot, it is necessary to design a mechanical structure suitable for different welding scenes, including the working range, force analysis and kinematics analysis of the equipment[5]–[8].

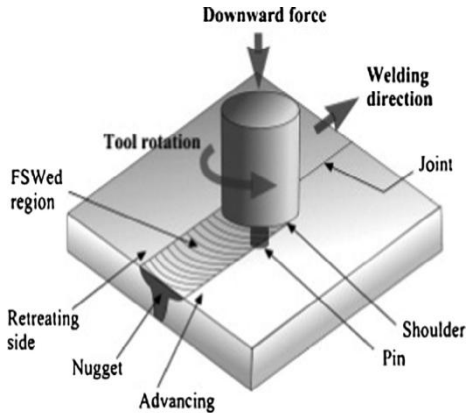

Figure 1: Technical principle of friction stir welding

The technical principle of friction stir welding is shown in Figure1. Firstly, a cylindrical, special agitating tool with a shoulder is rotated and slowlyinserted into the workpiece to be welded at a very high speed.During the high-speed rotation process, a large amount of frictional heat will be generated, which can thermally plasticize the material of the workpiece to be welded, and the thermoplastic material is gradually transferred from the front to the rear under the rotation of the stirring tool, and is stirred. The friction and the upset action of the tool gradually form a solid phase joint by diffusion, which has a dense and stable property.

1. Main performance parameters of friction stir welding

The friction stir welding technology is more complicated than the conventional welding technology.

1.1. Main parameters affecting welding quality

The process parameters affecting the final weld quality are also numerous but not limited to: Spindle speed, feed rate, insertion depth, welding pressure, tool geometry, tool material, material flow behavior, joint design and preheating or Cooling[9], [10].

I. **Spindle Speed**. The appropriate speed refers to the following conditions; Desired weld strength and quality of the weldment: Higher quality of weld and strength can be obtained at high speed operations, Material to be welded: Hard material requires high speed operation, Size of weld: Large welds require low speed operation, Thickness of the work piece to be welded.

II. **Feed rate/Welding speed**. The welding speed of the friction stir welding is the feed speed value of the stirring head along the welding direction of the sheet during the welding process, and the value mainly depends on the thickness and type of the welding workpiece. At the same time, due to the actual production efficiency and process requirements, the value can be adjusted accordingly to meet the actual welding requirements.

III. **Insertion Depth**. The workpiece is placed on the backing plate. Therefore, in order to allow a certain adjustment space after the welding needle is inserted into the welding material, the distance between the shoulder of the stirring head and the surface of the welding workpiece is used to represent the insertion depth of the stirring head. This parameter is not more than 0.3mm when welding a plate with a small thickness, and not more than 0.5mm when welding a thick plate.

IV. **Welding pressure**. The welding pressure parameter mainly refers to the upsetting pressure generated by the stirring head to the axial direction of the welding workpiece during the friction stir welding. The value is determined by the following factors: the type of material of the welding workpiece, the shape of the stirring head and the stirring head insertion depth. This value is substantially unchanged when the material of the welding workpiece and the mixing head are determined. A constant pressure is also used in the process of friction stir welding.

V. **Tool Geometry**[10], [11]. The performance of FSW tools vary with the tool geometry. The tool generally has circular section except at the end where there is a threaded *probe* or more complicated flute, the junction between the cylindrical portion and the probe is known as the *shoulder*.

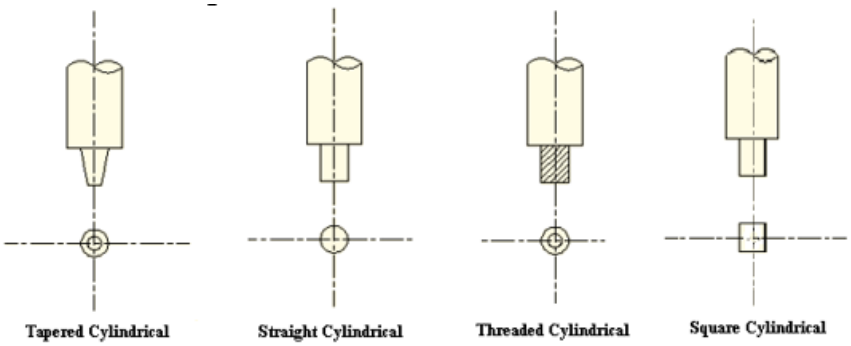

Figure2: Different FSW tool geometries

VI. **Tool material**. The tool material too greatly affects the quality of FSW. Generally used tool materials are high carbon steels with varying composition of other constituents such asChromium, Copper, and Nickel etc.

VII. **Preheating or Colling**. Preheating or cooling can also be important for some specific FSW processes. For materials with high melting point such as steel and titanium or high conductivity such as copper, the heat produced by friction and stirring may be not sufficient to soften and plasticize the material around the rotating tool. Thus, it is difficult to produce continuous defect-free weld. In these cases, preheating or additional external heating source can help the material flow and increase the process window. On the other hand, materials with lower melting point such as aluminum and magnesium, cooling can be used to reduce extensive growth of recrystallized grains and dissolution of strengthening precipitates in and around the stirred zone.

1.2. Stress analysis in Friction Stir Welding

When welding workpieces by friction stir welding, the most important influence on the welding quality is the bearing of the stirring head and the force on the stirring needle. The corresponding force analysis is not only helpful for improving the welding quality, but also it can increase the service life of the stirring needle and save costs. Therefore, it is necessary to correctly analyze these forces.The stirring needles are subjected to different forces in different welding stages, and are mainly divided into two stages of the insertion stage and the welding stage. The insertion phase refers to the process of rotating the mixing head into the welding workpiece, and the welding phase refers to the process of welding the workpiece when the mixing head is inserted to a suitable depth.

In the insertion stage of the mixing head during welding, the first contact with the workpiece to be welded is the stirring needle, and then the shoulder. At this time, the actual force of the stirring head is very complicated. In order to simplify the analysis, it is necessary to assume the direction of the stirring needle, the surface of the welded workpiece is vertical, and the welding material does not plastically move during the welding process, and the friction coefficient of the stirring needle is constant and the force is uniform. The structure of the mixing head is shown in Figure 3.

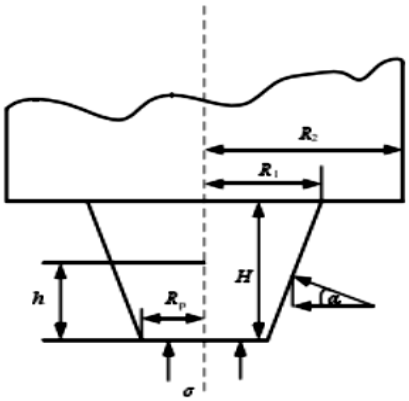

Figure 3: Structure of the mixing head

The positive pressure at the end of the agitating needle is known from:

$$N_{pb1} = \sigma_1.\pi R_p^2 (1)$$

Where; σ_1 . the positive pressure (MPa) of the stirring needle in the pressing stage
R_p . agitating needle end face radius in mm.
N_{pb1}.Rotating speedof the needle (Tool)

When the stirring head is inserted into the workpiece, the force is analyzed, and the side and end faces are subjected to a large resistance and the direction is upward. Since the contact surface is not smooth, frictional resistance is generated during the movement, thereby simultaneously generating a torque opposite to the direction of rotation of the friction stir welding. As shown in Figure 4.

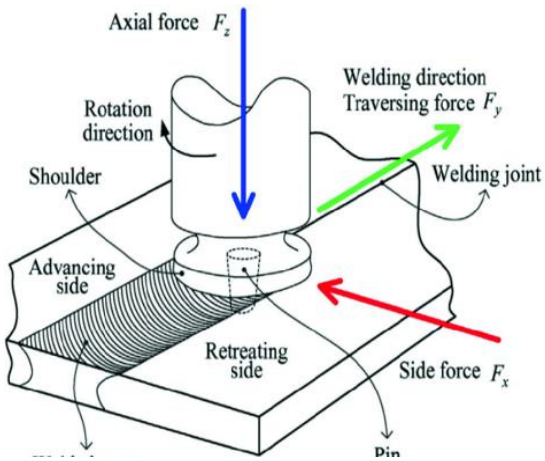

Figure4: Schematic diagram of the force at the welding stage[12]

P. Shahi et al[13] have expounded the forces in friction stir welding, as well as torque and power, induced by welding input parameters, including tool shape, material and process parameters, play a key role in welding. The dependent parameters in FSW are the forces and torque. The tool in the FSW process, due to its rotational and linear movement, experiences forces in three coordinate axis as shown in Figure 4.

- F_z : the z force, which is also named as the downward, forging, thrust or vertical force;The shoulder diameter affects the $F_z$strongly by a power of 2, according to the simplified equation as:

$$F_z = \pi . D^2 \cdot \frac{\sigma_y}{4} \quad (2)$$

$F_x$andF_y: the in-plane forces. $F_y$is also referred as the longitudinal/welding force/traverse force, which can be given by

$$F_y = \frac{2\pi \square (Mf - Mfo)}{C} \quad (3)$$

Where, C is the pitch of the ball screw and $\mu$is the transmission efficiency, the output torque of the$x$ -axis servo motor is the result of two acting forces: frictional force (f : between the ball screw and worktable that's total output torque-M_f, and the total torque while no traverse force-M_{fo}) and traverse force (F).Moreover, regarding the rotational movement, the torsional torque is exerted to the tool. The F_z,F_x, F_y and torque applied on the tool are analyzed.The total torque[13], can be computed from total shear stress as:

$$T = \oint r \times (\tau_t dA) = \tau_t \int_0^{R_s} 2\pi r^2 \, dr = \frac{2\pi R_s^{\ 2} \tau_t}{3}$$

Where the $\boldsymbol{\tau_t}$ is the total shear stress and R_s is the shoulder diameter. In addition, the spindle required power is computed as

$$P = \oint \{(1-\delta)\tau + \delta \mu_f P_N\} \omega r_A dA$$

Moreover, the tool force in the welding (y) direction results from two components, the force experienced by the tool shoulder (F_s) and the tool pin (F_p). Hence, the total force is given as

$$F = F_s + F_p \quad (6)$$

The shoulder and pin forces can be computed by using

$$F_S = \oint \delta \times \mu P \times dA \quad (7)$$

And

$$F_p = \oint \sigma \times dA \quad (8)$$

In these equations, **σ** is the yield strength of the base material considering the temperature of the workpiece and ***dA*** is the projected arc of the tool pin in the *y- z* plane. These analytical equations can be employed to calculate the force values for a given set of input parameters[13].

1.3. Design of the suggested friction stir welding parallel robot

1.3.1. Overall plan

Considering the insertion process of the stirring head at the beginning of the friction stir welding and the extraction process of the stirring head at the end of the welding, it is known that the robot is responsible for the movement of the electric spindle of the stirring head in the z-axis direction, and it is necessary to take into consideration that the stirring head is inserted to a certain angle of inclination, while also rotating according to the welding workpiece during the welding process, the robot also needs to have the freedom of rotation in the x-axis direction and the y-axis direction.

The forward, left and right movements during the welding process are realized using x-direction and y-direction slides. In combination with the force analysis of the above-mentioned mixing head during the insertion

process and the welding process, considering the actual welding process requirements, the robot needs to have the characteristics of strong bearing capacity and high rigidity.

Therefore, the 2UPR/RPS parallel structure is selected in the design. Structure design and thermal analysis of a new type of friction stir weld spindle[14].It can be seen from Figure 5, that the 2UPR/RPS parallel mechanism robot designed in this paper is mainly composed of a fixed platform, a moving platform and three driving branch rods. The fixed platform is mounted on the peripheral mechanical frame, and the movable platform and the fixed platform are connected by three driving branch rods. Its structural diagram is shown in Figure 6. The drive branch lever 1 and the drive branch lever 2 are composed of three joint pairs, respectively R, U, and P.

Where, in the R sub-axial directions are parallel to the two drive branch rods. The driving branch lever 3 is composed of three sub-groups, R pair, P pair and S pair. The R pair of the drive branch lever 3 and the R pair of the drive branch lever 1 are perpendicular to each other, and the R pair of the drive branch lever 3 and the R pair of the drive branch lever 2 are perpendicular to each other. The stir welding head of the friction stir welding is installed at the center of the moving platform.

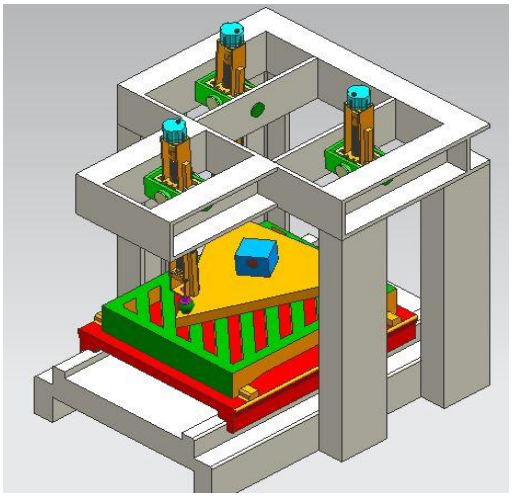

Figure 5: Schematic diagram of parallel friction stir welding robot

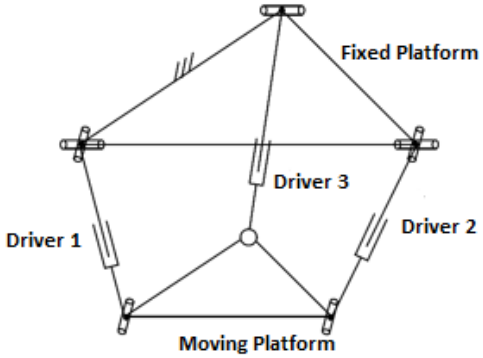

Figure 6: Schematic diagram of parallel robot structure

2.3.2. Coordinate system establishment

In order to facilitate the further analysis of the parallel mechanism, a coordinate system as shown in Figure 7, is established for it, which mainly includes two parts: a fixed coordinate system and a moving coordinate system.

The fixed coordinate system is on the plane of the fixed platform $A_1A_2A_3$, denoted as OXYZ, the origin position O is located in the middle of A_1A_2, the direction of the OA_3 is the X-axis direction of the coordinate system, and the direction of the ${}_OA_2$ is the Y-axis direction of the coordinate system, by the right hand, the rule can determine that the axis direction of the coordinate system is on the lower side perpendicular to the plane. The same principle is applied to establish the moving coordinate system oxyz on the plane of the moving platform. The origin position o is located in the middle of B_1B_2, the direction of oB_3 is the x-axis direction of the coordinate system, the direction of oB_2 is the y-axis direction of the coordinate system, and the z-axis is applied. The right hand rule is determined to be the lower side perpendicular to the plane $B_1B_2B_3$.

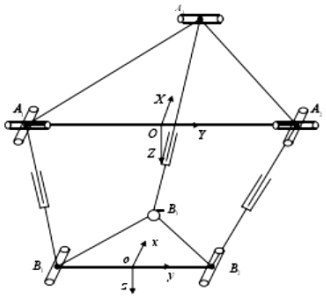

Figure 7: Parallel Robot Coordinate System

2.3.3. Degree of freedom analysis

Before the kinematics analysis, the number of spatial degrees of freedom of the parallel friction stir welding robot needs to be determined. Because the structure of the parallel robot is more complicated, there are many methods for solving the degree of freedom. The most widely used and accurate calculation method is the revised Grübler (1917) or Kutzbach (1929) criterion.

$$F = \lambda (n - j - 1) + \sum_i^j fi (9)$$

Where:

F: degree of freedom of a mechanism.

f_i: degree of relative motion permitted by joint i.

j: number of joints in a mechanism, assuming that all the joints are binary.

λ: degree of freedom of the space in which a mechanism is intended to function. Hence λ =6 for spatial mechanisms and λ = 3 for planar and spherical mechanisms.

$$\lambda = c_i + f_i (10)$$

c_i:number of constraints imposed by joint i.

n:number of links in a mechanism, including the fixed link.

Therefore, to determine the number of degrees of freedom of the parallel robot in this design, the parameter values in the formula in turn have to be solved. The total number of components in the parallel mechanism n=8 can be obtained through Figure 6: λ = 3, j =9 (2 U pairs, 3 R pairs, 3 P pairs, 1 S pair),$\sum_i^j fi = 9$.

Substituting the obtained parameter values into the modified Grübler (1917) or Kutzbach (1929) criterion:

$$F = \lambda (n - j - 1) + \sum_i^j fi;\ F = 3(8-9-1) + 9 = 3 \quad (11)$$

It can be seen from the above calculation that the 2UPR/RPS parallel mechanism used in this paper has three degrees of freedom. Further analysis shows that the three degrees of freedom of the mechanism in the initial position are the rotational degrees of freedom in the Y-axis direction of the bound coordinate system, and the orbiting coordinates. The degree of freedom of rotation in the X-axis direction and the degree of translational freedom in the Z-axis direction.

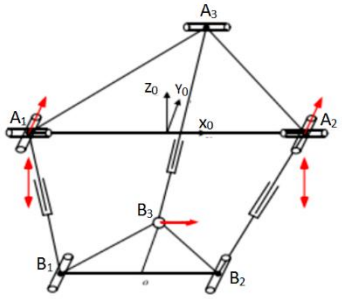

Figure 8: Schematic diagram of the binding force of the parallel robot

Among them, the red arrow in Figure 8, indicates the direction of the binding force and the binding couple.

2.3.4 Kinematics analysis

From the two main types of kinematics analysis of robots, one of which is positive or direct kinematics and the other is inverse kinematics. In (L.W, 1999), Tsai introduced both kinematics solution for different manipulators. The positive kinematics method is explained as: Forward kinematics requires the limb lengths to be given and the position and orientation of the mechanism to be found. The pose state during the motion of the robot is solved according to the known conditions.The Inverse kinematics method is explained as: The independent variables are given; the problem is to find the limb lengths.Hence the position and orientation of the moving platform will be completely known. Then, the state of the end moving rail mechanism of the robot is solved according to this known condition.

The FSW parallel robot designed in this paper, the inverse kinematics solution is easier to obtain, and the positive kinematics solution is relatively complicated. Therefore, the inverse kinematics of the parallel robot is analyzed and taken for the design development.

Euler angles and coordinate transformation matrix tools are used in the process.The initial position of the parallel mechanism in the moving coordinate system oxyz is: First, $[X_0, Y_0, Z_0]^T$, which is used to obtain the constraint equation of each driving branch. Through the size and length of the fixed platform and the moving platform in the mechanism, as shown in Figure 9, the coordinates of the end points of the driving branch rod are obtained.

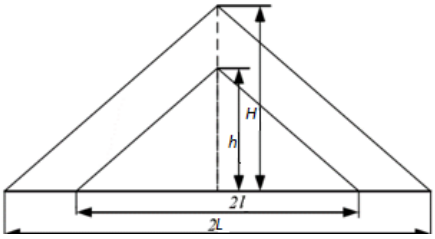

Figure 9: Structure of the fixed platform and moving platform of the parallel mechanism.

Considering Figure 7, let A_i and ${}^{B}B_i$ be the position vectors of points A_i and B_i in the coordinate systems A and B, respectively. Then the coordinates of A_i and B_i are;

$$\begin{Bmatrix} A1 = [0, -l, 0]T \\ A2 = [0, l, 0]T \\ A3 = [h, 0, 0]T \end{Bmatrix} (12)$$

$$\begin{Bmatrix} B1 = [0, -L, 0]T \\ B2 = [0, L, 0]T \\ B3 = [H, 0, 0]T \end{Bmatrix} (13)$$

WhereB_i in the determined coordinate system are based on the rotation matrix **R** to convert the moving platform coordinate system to the fixed platform coordinate system, expressed as

$${}^{A}B_i = {}^{A}R_B\, B_i, \text{ where i = 1, 2 and 3} \quad (14)$$

From the knowledge of robotics, the rotation matrix used to convert the moving platform coordinate system to the fixed platform coordinate system is given by:

$$R(\psi, \Theta, \phi) = R(z, \psi)\, R(y, \Theta)\, R(x, \phi)$$

$${}^{A}R_B = \begin{bmatrix} ux & vx & wx \\ uy & vy & wy \\ uz & vz & wz \end{bmatrix} = \begin{bmatrix} u11 & v12 & w13 \\ u21 & v22 & w23 \\ u31 & v32 & w33 \end{bmatrix} = \begin{bmatrix} c\phi c\theta & c\phi s\theta s\psi - s\phi c\psi & c\phi s\theta c\psi + s\phi s\psi \\ s\phi c\theta & s\phi s\theta s\psi + c\phi c\psi & s\phi s\theta c\psi - c\phi s\psi \\ -s\theta & c\theta s\psi & c\theta c\psi \end{bmatrix} (15)$$

Where: C= Cosine and s= Sin, and ϕ, θ, Ψ are rotation angles about x, y and z-axes, known as roll, pitch and yaw.Hence, six variables completely define the position and rotation of a moving platform are.

$$X = [P_x P_y P_z \phi \quad \Theta \quad \psi]^T$$

Where x_i, $y_i$and z_i are the final positions after the transformations. The above denote the positions of the end-effector $b_i(x_i, y_i, z_i)$ for i= 1, 2, 3and *w* is the translation along the *Z-axis* (The extension of the linear actuator).

Since $\theta = 0$ or π in the rotation matrix R, when $\theta = 0$, there are:

$$^{A}R_{B} = \begin{bmatrix} c\phi & -s\phi c\psi & s\phi s\psi \\ s\phi & c\phi c\psi & -c\phi s\psi \\ 0 & s\psi & c\psi \end{bmatrix} \quad (16)$$

The element of $^{A}R_{B}$ must satisfy the given orthogonal conditions. The position vector qi and Bi with respect to the fixed coordinate system is obtained by the following transformation[15]:

$$q_i = P + {}^{A}R_{B}\, B_i \quad (17)$$

Substituting Eqs. (12), (13) and (15) into (17) yields the values of q_1, q_2 and q_3.
Length of Limb i, as thedrivers (d_i), shown in Fig. 6, is given by

$$d_i^2 = [q_i - a_i]^T [q_i - a_i] \qquad \text{for i = 1, 2, 3.} \quad (18)$$

By substituting the values of q_i and Eq. (12) into (18) yields the value of d_i, d_2 and d_3 which are the lengths of the three limbs of the mechanism. And by expanding the right hand side of Eq. (18) and taking the square root yields[16];

$$d_i = \pm\sqrt{(P_x + b_{ix} - a_{ix})^2 + (P_y + b_{iy} - a_{iy})^2 + (P_z + b_{iz} - a_{iz})^2}$$

Though the equation shows two possible solutions for the manipulator position, only the positive limb length can be obtained without changing the configuration of the manipulator.

II. Conclusions

The mechanical structure of this parallel FSW robot proposed to be designed and tested for manufacturing of different weld quality with free-defect, low cost, capable to join high strength materials by maintaining the tool movements with no tool deviation as force accumulated during the welding process will be fully controlled.

However, the parallel design gains in stiffness but has a complex Cartesian workspace, significantly less flexibility. It is more suited to applications where the parts are relatively small, multi axis capability is required, and the force requirements are a little higher than what the Serial Kinematic Robot is able to generate. This mechanism can also be considered where, thematerialcanbeweldednearorclosetothehorizontal plane and where the higherforceorstiffnessaresome- what required.Higher forces and increased stability can be reached with this kinematics robots.

A good way to handle the drawback by using force control system which using a force sensor to measure the real force and send it back as a reference force so that correct the input force is studied.In this paper, the process parameters of friction stir welding and the force analysis of the stirring head during welding are studied and discussed. Then the overall structural scheme of the parallel mechanism robot is established, and the establishment of the coordinate system, the solution of the degree of freedom, and the kinematics are proven. The inverse solution is analyzed to lay the theoretical foundation for the next force motion control.

References

[1]. M. Soron and I. Kalaykov, "A Robot Prototype for Friction Stir Welding," 2006.
[2]. D. S. Zhang, Y. D. Xu, J. T. Yao, and Y. S. Zhao, "Analysis and Optimization of a Spatial Parallel Mechanism for a New 5 – DOF Hybrid Serial – Parallel Manipulator," *Chinese J. Mech. Eng.*, pp. 1–9, 2018.
[3]. T. Handbook, "Friction Stir Welding."
[4]. N. Mendes, P. Neto, A. Loureiro, and A. Paulo, "Machines and control systems for friction stir welding : A review," *JMADE*, vol. 90, pp. 256–265, 2016.
[5]. L. U. O. Hai-, "Mechanical analysis of friction stir welding robot under typical working conditions," 2015.
[6]. G. Zhuang and A. Region, "Friction Stir Welding Technology," pp. 75–79, 2012.
[7]. Ş. Staicu, "Inverse dynamics of the spatial 3-," vol. 13, no. 1, pp. 62–70, 2012.
[8]. *SERIAL AND PARALLEL ROBOT MANIPULATORS*. .
[9]. P. Tanwar and V. Kumar, "Friction Stir Welding : Review," vol. 3, no. 10, pp. 172–176, 2014.
[10]. V. Gupta, "I DENTIFING P ARAMETERS A FFECTING F RICTION," no. January 2013, 2017.
[11]. D. Raguraman, D. Muruganandam, and L. A. Kumaraswamidhas, "STUDY OF TOOL GEOMETRY ON FRICTION STIR

WELDING OF AA 6061 AND AZ61," pp. 63–69, 2014.
[12]. P. Welding, *Polymer Welding Techniques and Its*, no. c. 2019.
[13]. P. Shahi and M. Barmouz, "Force and Torque in Friction Stir Welding," no. April, 2016.
[14]. H. Luo, L. Xiao, J. Wu, H. Zhang, and W. Zhou, "Structure design and thermal analysis of a new type of friction stir weld spindle," vol. 9, no. 5, pp. 1–14, 2017.
[15]. "The Mechanics of Serial and Parallel Manipulators.pdf." .
[16]. L. B. Ila, "Design and Development of a 3-Degree of Freedom Parallel Manipulator," 2014.

Nicas January Benard,etal. "Structure Analysis of Parallel Robot in Friction Stir Welding Technology."*IOSR Journal of Mechanical and Civil Engineering (IOSR-JMCE)*, 17(2), 2020, pp. 11-19.